

# Metasomatic Alterations of Olivine Inclusions in the Budulan Mesosiderite

C. A. Lorenz<sup>a</sup>, M. A. Nazarov<sup>a</sup>, F. Brandstaetter<sup>b</sup>, and Th. Ntaflos<sup>c</sup>

<sup>a</sup> Vernadsky Institute of Geochemistry and Analytical Chemistry, Russian Academy of Sciences,  
ul. Kosygina 19, Moscow, 119991 Russia

e-mail: c-lorenz@yandex.ru

<sup>b</sup> Naturhistorisches Museum, A-1014 Wien, Burgring 7, Österreich

e-mail: franz.brandstaetter@NMH-WIEN.ac.at

<sup>c</sup> Department für Lithosphärenforschung, Universität Wien, Althanstrasse 14, 1090 Wien, Österreich

e-mail: theodoros.ntaflos@univie.ac.at

Received February 25, 2010

**Abstract**—Mesosiderites are thermal metamorphic breccias consisting of fragments of pyroxene–plagioclase rocks and FeNi metal. The silicate constituent of mesosiderites has a chemical and oxygen isotopic composition analogous to those of meteorites of the HED group: howardites, eucrites, and diogenites. The hypothesis currently most widely accepted for the genesis of mesosiderites is the impact mixing of the material of a differentiated asteroid and an iron meteorite. In contrast to many other classes of meteorites, mesosiderites exhibit no traces of metasomatic processes. The Budulan mesosiderite is the first meteorite of this type in which traces of metasomatism under the effect of an anhydrous fluid were detected. The metasomatic alterations are manifested as chemical zoning of olivine, aggregates of secondary minerals, and the mobilization and redeposition of iron and nickel in the form of metals and sulfides. These alterations were most probably caused by a reaction of olivine with S- and/or CO-bearing gases of endogenic or supergenic provenance. Traces of such metasomatic alterations were previously found in some meteorites and lunar rocks, and these processes could likely play a certain role in the differentiation of chondritic bodies.

**DOI:** 10.1134/S0869591110050012

## INTRODUCTION

Mesosiderites are stony-iron meteorites containing commensurable amounts of silicates and FeNi metal. The chemical composition and oxygen isotopic ratios (Clayton and Mayeda, 1996) of their silicates correspond to those of HED meteorites (howardite–eucrite–diogenite). The metal phase of mesosiderites is close in chemical composition to iron meteorites of group IIIAB (Wasson et al., 1974). It is currently thought that mesosiderites were formed on the differentiated parent body during its catastrophic collision with iron asteroids and the resultant mixing of silicate rock fragments and molten metal (Wasson and Rubin, 1985).

The Budulan mesosiderite has a mass of close to 100 kg and was found in Buryatia, Russia, in 1962. Kirova and D'yakonova (1966) published the first descriptions of its mineralogy, petrography, and chemical composition. Budulan is a highly metamorphosed mesosiderite of group 3B and has a poikiloblastic texture (Floran, 1978). It was, however, later demonstrated (Hewins, 1984) that the silicate component of mesosiderites of group 3B provides textural evidence of their crystallization from melt and that they should be classed with group 4B. The mesosiderites of this

group have a poikilitic texture of their plagioclase oikocrysts and pyroxene chadacrysts and are distinguished for elevated contents of orthopyroxene and olivine compared to those in other mesosiderites.

The source of mesosiderites and other meteorites of group HED is a relatively large differentiated body, perhaps, the asteroid Vesta (see, for example, Gaffey, 1997), whose mantle may consist of olivine. It is thus interesting to examine olivine fragments in the silicate constituent of such meteorites.

Olivine is contained in mesosiderites in an amount of close to 5 vol % (Delaney et al., 1980). The composition of the olivine is  $Fo_{55-93}$  at  $Fe/Mn = 40-55$  at (Goodrich and Delaney, 2000). The  $FeO/MnO$  ratio of olivine in mesosiderites was determined (Delaney et al., 1980) to decrease with increasing Mg# of the mineral, which is possibly explained by partial Fe reduction. The most magnesian olivine in mesosiderites occurs as inclusions of the composition  $Fo_{92-93}$  (Ntaflos et al., 1993; Boesenbergs et al., 1997; Terribilini et al., 2000; Wasson and Rubin, 1985).

Although olivine inclusions in the Budulan mesosiderite were found and documented by Kirova and D'yakonova (1966), several researchers (Floran, 1978; Prinz et al., 1980a) later failed to identify olivine in

Average compositions (wt %) of olivine and pyroxene in olivine inclusions in the Budulan mesosiderite

Inclusion type/mineral	Na <sub>2</sub> O	MgO	Al <sub>2</sub> O <sub>3</sub>	SiO <sub>2</sub>	K <sub>2</sub> O	CaO	TiO <sub>2</sub>	Cr <sub>2</sub> O <sub>3</sub>	MnO	FeO	Total	Fo	En	Wo	Fe/Mn
<i>Low-Mg olivine inclusion B1/98</i>															
Unaltered olivine	n.d.	29.8	0.03	37.5	0.03	0.06	0.17	0.18	0.72	31.4	99.9	62.9			43
Strongly altered olivine	n.d.	36.6	n.d.	39.4	0.06	0.02	0.08	0.08	0.76	22.0	99.0	74.8			28.5
Pyroxene replacing olivine	n.d.	26.0	0.13	48.3	n.d.	0.10	0.08	0.16	0.82	23.3	99.8	66.5	0.18		28
<i>High-Mg olivine inclusion B3/99</i>															
Unaltered olivine	n.d.	46.9	n.d.	40.7	n.d.	0.03	n.d.	0.03	0.29	12.9	100.9	86.6			44.9
Orthopyroxene inclusion in olivine	0.08	29.6	1.36	53.8	n.d.	0.74	0.11	4.57	0.43	10.8	101.5		81.8	1.47	24.8
Orthopyroxene in chromite–pyroxene symplectite	0.32	28.4	0.42	57.0	n.d.	0.79	0.47	0.73	n.d.	11.9	100.1		79.7	1.6	
Clinopyroxene in chromite–pyroxene symplectite	0.95	16.8	0.93	52.1	0.03	25.3	0.08	1.01	0.52	3.02	100.5		45.8	49.6	5.73
Strongly altered olivine	n.d.	53.4	n.d.	42.9	n.d.	n.d.	n.d.	n.d.	0.17	2.55	99.0	97.4			14.8
Pyroxene replacing olivine	n.d.	35.6	0.16	55.1	n.d.	0.25	0.03	0.1	0.37	6.23	97.8		90.7	0.46	16.6

Note: n.d. means no detected.

this meteorite. Our preliminary studies (Lorenz et al., 1999, 2000) confirmed that the Budulan mesosiderite does contain olivine fragments. The olivine inclusions turned out to show evidence of “dry” metasomatism, a process that have never before been detected in any mesosiderites. This paper presents our results obtained by studying such inclusions. We also discuss the possible role of metasomatic processes in the history of the parent body of mesosiderites.

## MATERIALS AND METHODS

In order to study olivine inclusions in the Budulan mesosiderite, we prepared 15 polished sections of samples of this meteorite. Olivine inclusions were identified only in three of these sections. In addition, we examined selected fragments of large olivine inclusions from the groundmass, which were obtained during the laboratory processing of the meteorite material and then used to prepare polished thin sections. The thin sections were examined under an optical microscope at the Vernadsky Institute and under an JSM 6400 scanning electron microscope at the Natural History Museum in Vienna (NHMW). The chemical composition of phases was analyzed on various microprobes: Camebax Microbeam (at the Vernadsky Institute), ARL-SEMQ (at NHMW), and Cameca SX-100 (at the Department of Lithospheric Studies of the Vienna University). The Ni and Co concentrations of the metallic phase in the meteorite were determined by instrumental neutral activation analysis at the Vernadsky Institute.

## RESULTS

The Budulan meteorite is made up of polymictic metabreccia consisting of fragments of pyroxene, plagioclase, and pyroxene–plagioclase rocks with evenly distributed FeNi metal segregations (~50 vol % of the rock) in between (Fig. 1a). The silicates are not zonal in both clasts of pyroxene–plagioclase rocks and monomineralic fragments. The composition of the pyroxene varies from  $En_{55}Wo_{1-5}$  to  $En_{73}Wo_{1-5}$  ( $Fe/Mn \approx 30$ ) (Fig. 2a), and the plagioclase is  $An_{79}-An_{96}$ . The metallic phase is kamacite (5.2 wt % Ni,  $Ni/Co \approx 13$ ) with taenite inclusions (30–50 wt % Ni). The average Ni concentration in the metal accounts for 8.55 wt % ( $Ni/Co \approx 18$ ). Large metal segregations are connected by a network of veinlets 10–50  $\mu m$  thick, which consist of kamacite, taenite, and schreibersite. The accessory minerals are chromite, silica, merrillite, troilite, ilmenite, rutile, Ca, Mg, Fe, and Mn phosphates, and fayalite.

Olivine inclusions account for approximately 5 vol % of the meteorite, have sharp contacts with the host rocks (without associated zoning), and can be classified into high-Mg ( $Fo_{62}$ ) and low-Mg ( $Fo_{86}$ ) groups (table).

The low-Mg inclusions are 0.5–5 mm across and consist of olivine ( $Fo_{62}$ ,  $Fe/Mn \approx 45$ ) with occasional inclusions of low-Ca pyroxene, troilite, and FeNi metal (2.4 wt % Ni). The inclusions are cut across by troilite (0.4–1.6 wt % Ni) veinlets and are variably replaced by  $Fe^{3+}$  hydroxides, which were synthesized in the course of oxidation on the Earth’s surface. Some troilite veinlets intersect the boundaries of the inclusions and continue in the host mesosiderite rock (Fig. 1e). The Mg# of olivine around the veinlets increases from  $Fo_{62.9}$  to  $Fo_{74.8}$  toward the planes of the veinlets (Fig. 2b). The Fe/Mn ratio simultaneously

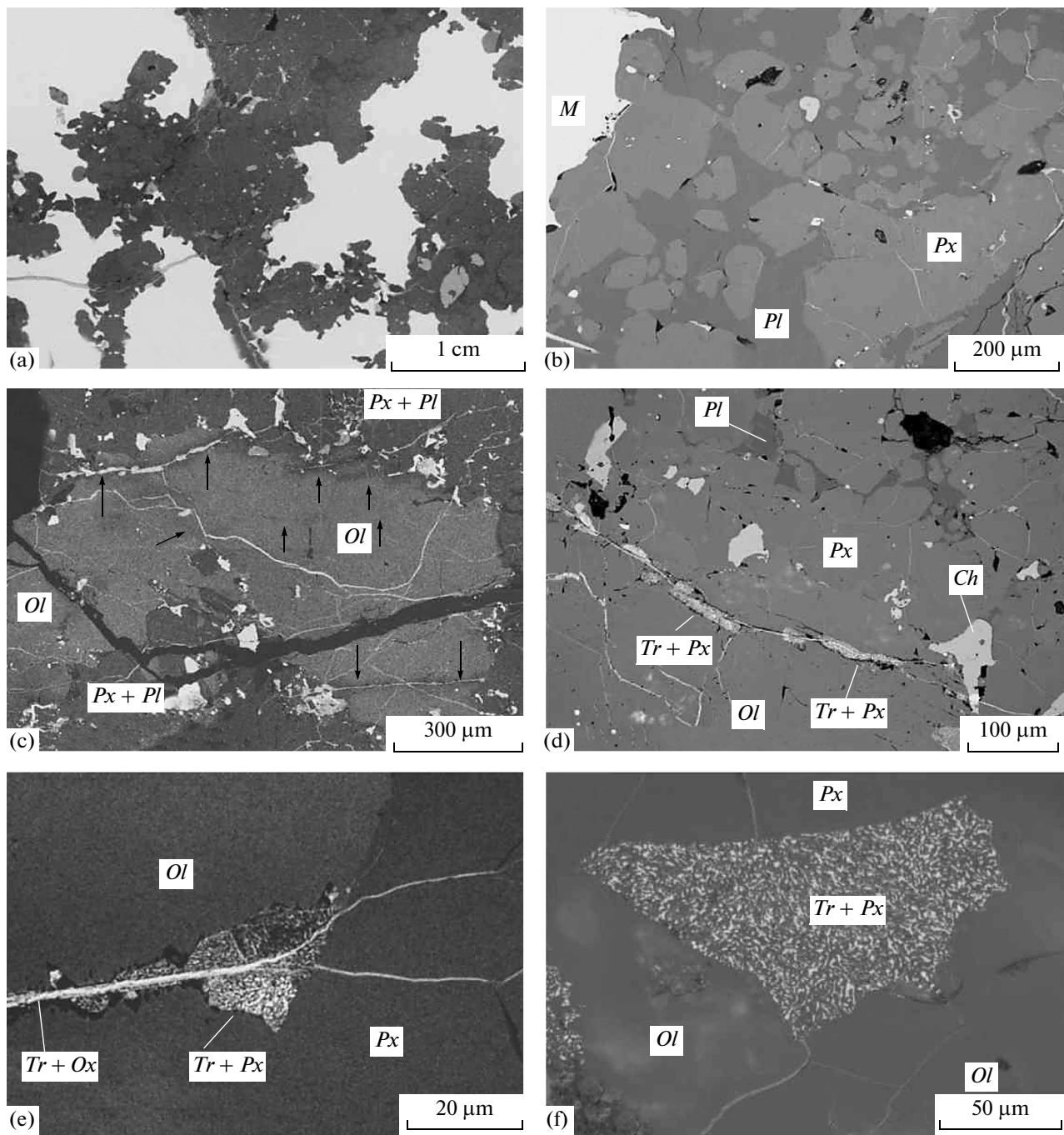


**Fig. 1.** Textures of the Budulan mesosiderite and secondary mineral aggregates in its low-Mg olivine inclusions.

(a) Texture of the Budulan mesosiderite: white—metal, gray—silicates; (b) poikiloblastic texture of the silicate constituent of the mesosiderite: *M*—metal, *Px*—pyroxene, *Pl*—plagioclase; (c) low-Mg olivine inclusions in the Budulan mesosiderite. Arrows point to fractures with darker zones of secondary alterations around them and fine-grained troilite-pyroxene aggregates replacing olivine (*Ol*); (d) troilite veinlet (it is extensively replaced by Fe hydroxides) in a low-Mg olivine inclusion with zones of secondary alterations, in which olivine is replaced by troilite and pyroxene aggregates: *Tr*—troilite, *Ch*—chromite; (e) veinlet cutting across a contact of a low-Mg olivine inclusion and matrix pyroxene. The veinlet is filled with troilite, which is extensively replaced by Fe hydroxides (*Ox*). The domain in which olivine is replaced by a troilite-pyroxene aggregate is truncated by matrix pyroxene; (f) troilite and pyroxene aggregate at a boundary of a low-Mg olivine inclusion and the groundmass of the mesosiderite. All images in Figs. 1–4 are micrographs taken under an optical microscope, except Figs. 1a, 1c, 1e, 3a, 4b, and 4c, which are BSE images.

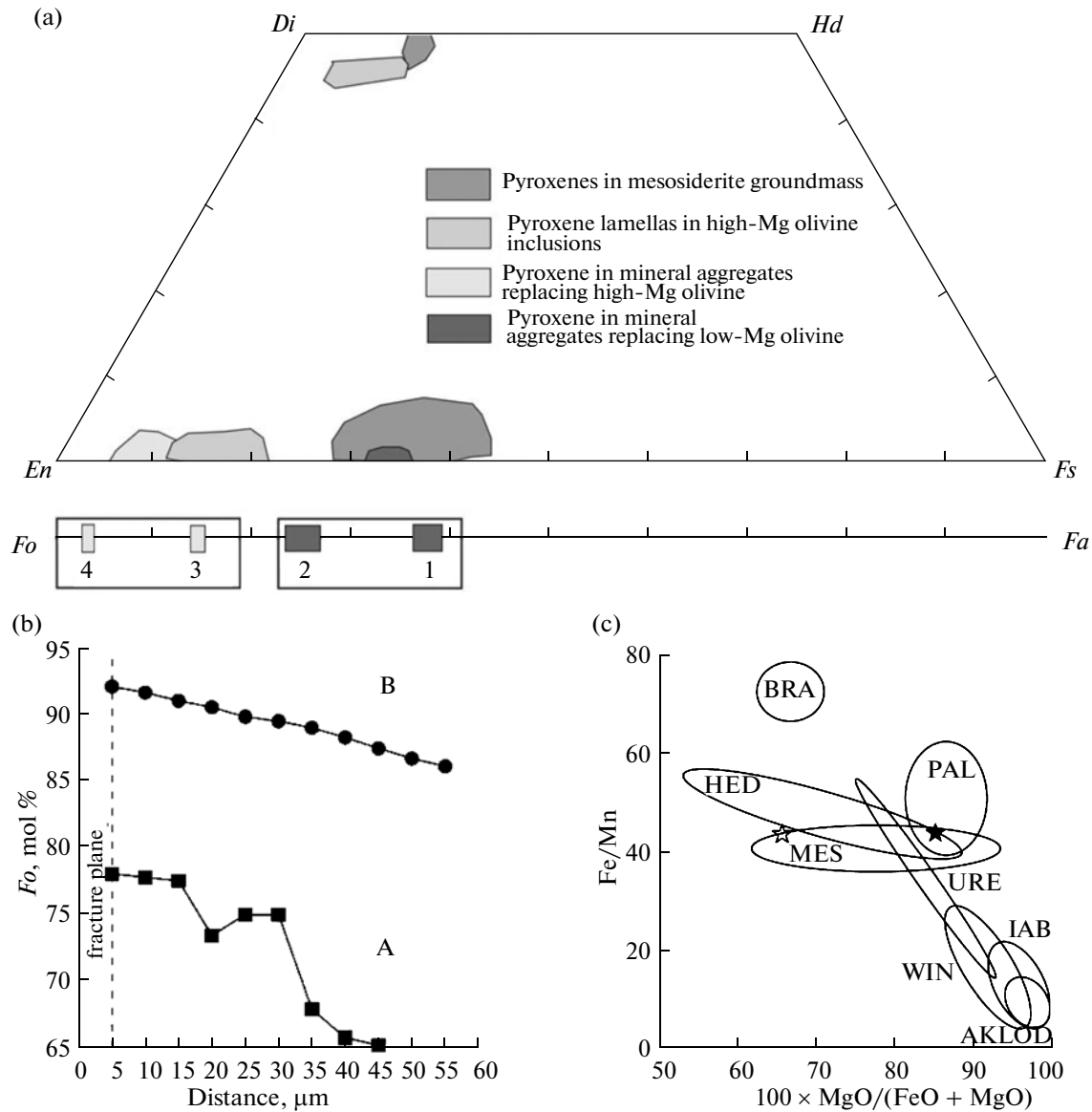


**Fig. 2.** Olivine and pyroxene compositions in the Budulan mesosiderite.

(a) Olivine and pyroxene compositions (mol %): (1, 2) compositions of unaltered and reduced olivine in low-Mg inclusions; (3, 4) compositions of unaltered and reduced olivine in high-Mg inclusions; (b) olivine zoning in secondary alteration zones around fractures in olivine inclusions. The left-hand part of the profile shows olivine near the fracture, and the right-hand part corresponds to unaltered olivine. A—low-Mg olivine inclusions, B—high-Mg olivine inclusions; (c) Mg# and FeO/MnO (mol %) ratios of olivine (the open and solid stars indicate unaltered olivine in low- and high-Mg olivine inclusions, respectively) and meteorites of other groups (data from *Planetary Materials*, 1998): AKLOD—acapulcoites and lodranites; BRA—brachinites (Mittlefehldt, 2003); HED—howardites, eucrites, and diogenites; IAB—silicate inclusions in IAB iron meteorites; MES—mesosiderites; PAL—pallasites; URE—ureilites; WIN—winonaites (Prinz et al., 1980b).

decreases from 45 to 30. Along these veinlets (Figs. 1c–1e) and, occasionally, at contacts between olivine inclusions and the host mesosiderite rock (Fig. 1f), olivine may locally contain aggregates of troilite and low-Ca  $En_{64-70}$ .

The high-Mg inclusions are notably larger (1.5–3 cm) and consist of subhedral olivine grains ( $Fo_{86}$ ,  $Fe/Mn \approx 46$ ) 3–5 mm across. These inclusions occasionally contain narrow (10–30  $\mu\text{m}$ ) and long (up to

5 mm) orthopyroxene lamellae ( $En_{85-89}Wo_{1.0-2.5}$ ;  $Fe/Mn \approx 36$ ) bearing fine-grained graphic intergrowths (symplectites) of chromite and orthopyroxene (Fig. 3a) with rare inclusions of troilite, plagioclase ( $An_{99}$ ), orthopyroxene ( $En_{49.35}Wo_{45.74}$ ), and FeNi metal (1.1–3.3 wt % Ni). The olivine grains contain relatively large (50–100  $\mu\text{m}$ ) single irregularly shaped inclusions of troilite (Fig. 3b), metallic iron, Ca phosphate (merrillite), and chromite.

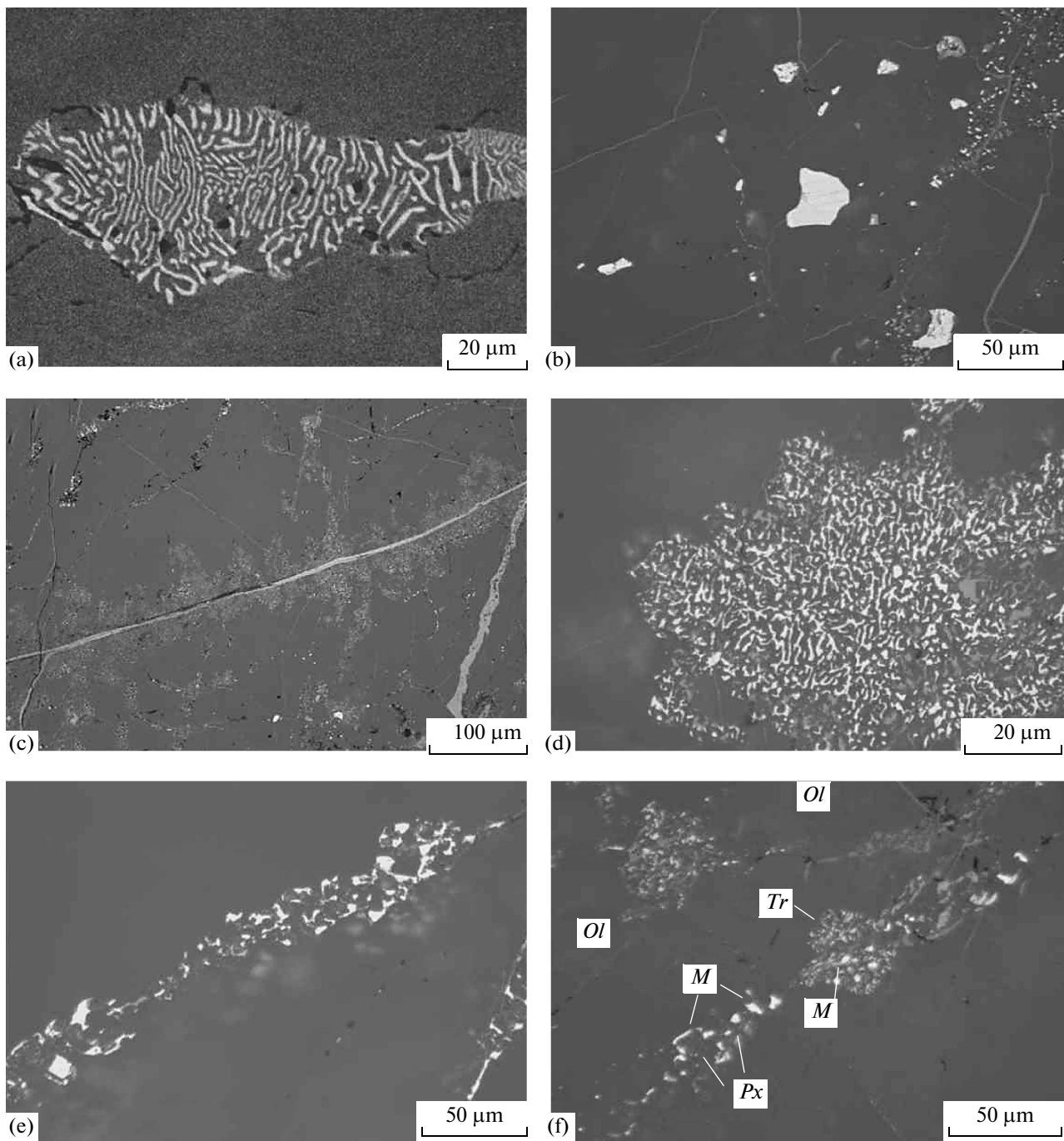


**Fig. 3.** Textures and mineral morphologies in high-Mg inclusions in the Budulan mesosiderite.

(a) Fine-grained symplectitic aggregate of chromite (pale gray) and orthopyroxene (dark gray) in high-Mg olivine; (b) troilite inclusion in olivine; (c) olivine replacement by an aggregate of secondary minerals along thin veinlets around a broad fracture; (d) olivine replacement by an aggregate of secondary troilite, pyroxene, and silica; (e) aggregate of metal and pyroxene in a portion of a vein filled with FeNi metal; (f) development of metal-silicate and troilite-silicate aggregates along the same fracture.

Long (up to 200  $\mu\text{m}$ ) fractures along boundaries of olivine in the high-Mg inclusions are filled with Fe hydroxides (6.2 wt % NiO) with angular olivine fragments and inclusions of chromite, anorthite ( $An_{99}$ ), and merrillite and with relics of kamacite (5 wt % Ni, Ni/Co = 5–15) and taenite (54 wt % Ni). In some

fractures, FeNi phosphate develops along contacts between olivine and Fe hydroxides. The composition of the phosphate is close to that of arupite ( $\text{Ni}, \text{Fe}^{2+})_3(\text{PO}_4)_2 \cdot 8\text{H}_2\text{O}$ ). Larger fractures are accompanied by arrays of thin subparallel fractures with veinlets of troilite and metallic iron intensely replaced by Fe and

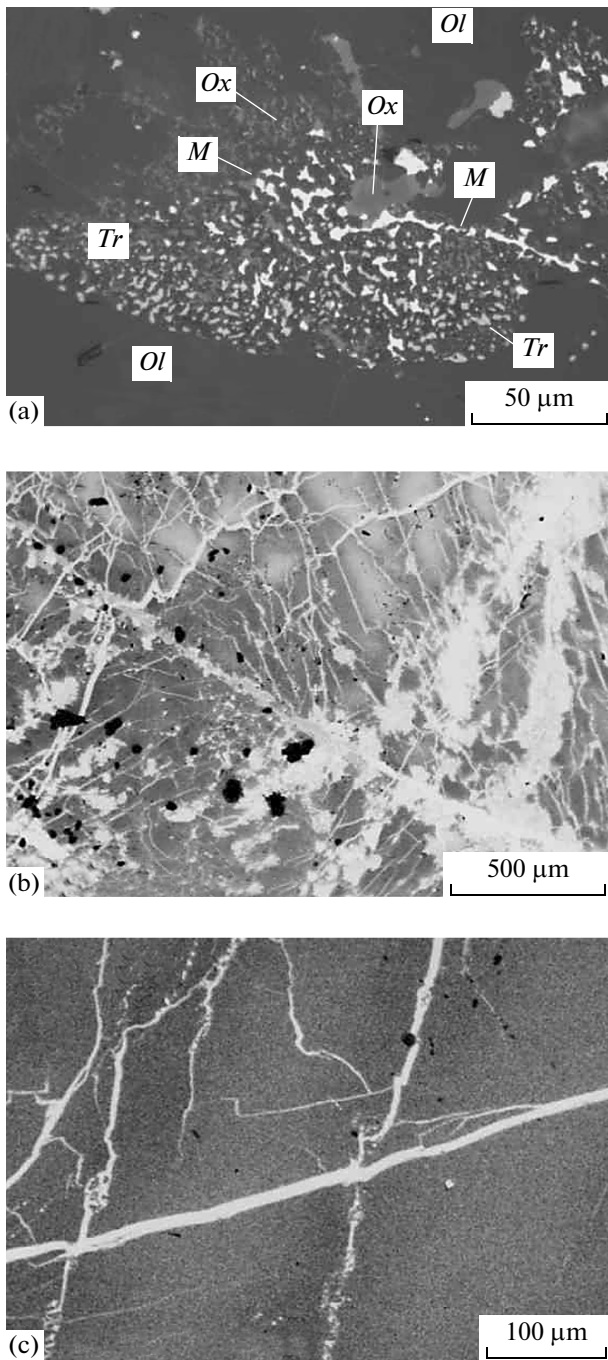


**Fig. 4.** Relations between secondary mineral aggregates of various types in a high-Mg olivine inclusion in the Budulan mesosiderite.

(a) Veinlet filled with metal intrudes a zone of troilite-silicate aggregates and forms a metal-troilite-silicate aggregate; (b) strongly altered domain in a high-Mg inclusion. An aggregate of troilite and silicates (white) replaces olivine (gray). Thin veinlets are contoured by zones of elevated Mg# (dark gray) that grade into a domain of unaltered olivine (pale gray); (c) troilite veinlet cutting across alteration zones (dark gray) in olivine (pale gray).

Ni hydroxides. As in low-Mg olivine inclusions, the Mg# of olivine increases from  $Fo_{86}$  to  $Fo_{97}$  toward the planes of fractures (table, Figs. 2b, 4b), and the Fe/Mn ratio simultaneously decreases from 46 to 15. Veinlets are locally accompanied by discontinuous rims of fine-grained polymineralic aggregates of various types (Figs. 3c, 4b). Their zones become continuous around the thickest and longest fractures.

The most common aggregates are sulfide-pyroxene-silica (type I), which consist of 1–5  $\mu\text{m}$  grains of Fe sulfides, pyroxene  $En_{90.7}Wo_{0.4}$  ( $\text{Fe}/\text{Mn} \approx 17$ ) (Fig. 1f) and silica (Fig. 3d). Silica grains are localized in the interstices of pyroxene and sulfide grains and never occur in immediate contact with nearby olivine. The aggregates replace olivine within zones 100  $\mu\text{m}$  thick along fractures. The aggregates of type II, which are spread much less widely, consist of sulfide, metal, pyroxene, and silica and contain 5–15 vol % FeNi metal. The aggregates of type III (metal-pyroxene-silica) consist of 5- to 15- $\mu\text{m}$  metal grains, pyroxene, and silica and develop around single thin metal veinlets as rims 10–20  $\mu\text{m}$  thick (Fig. 3e). Aggregates of these types usually systematically alternate along a single veinlet (Fig. 3f). The Ni concentrations in the polymineralic aggregates of types I and II vary from 1.5 to 52.8 wt %, similar to the composition of sulfides in veinlets cutting across the olivine. Ni-poor and Ni-rich sulfides may locally coexist. The sulfides and metal are ubiquitously replaced by Fe hydroxides with 2.5–8 wt % NiO and 0.5–12 wt %  $\text{SiO}_2$ . The oxidized veinlets rimmed by fine-grained aggregates often contain grains of metal, sulfide, and, more rarely, silica and chromite.

Olivine inclusions show traces of kink deformations of impact or tectonic genesis. Neither increase in the Mg# of the olivine nor development of polymineralic aggregates were detected near younger metal and sulfide veinlets that cut across all of the aforementioned textural features and host olivine (Fig. 4c).

## DISCUSSION

### Sources of Magnesian Olivine

The Mg#, Fe/Mn ratio (30), and  $\text{Cr}_2\text{O}_3$  and  $\text{CaO}$  concentrations of orthopyroxene in the Budulan mesosiderite are analogous to those of pyroxenes in other mesosiderites (Mittlefehldt, 1979) and HED meteorites (Ruzicka et al., 1997). The rocks composing the silicate constituent of this meteorite are likely analogues of orthopyroxene cumulus eucrites (Delaney, 1984; Mason, 1994).

The low-Mg olivine inclusions contain olivine  $Fo_{62}$  ( $\text{Fe}/\text{Mn} \approx 45$ ), whose composition corresponds to that of olivine occasionally found in HED meteorites (Fig. 2c). Olivine ( $Fo_{60}$ ) is the first liquidus phase to crystallize from eucrite melts (Stolper, 1977), and hence, it is reasonable to suggest that the possible source of the low-Mg olivine could be the cumulus

rocks of eucrite magmas. The high-Mg olivine ( $Fo_{86}$ ), which does not crystallize from eucrite melts, requires another source. The Fe/Mn ratio of high-Mg inclusions in Budulan are the same as in olivine in HED meteorites and differs from olivine of primitive achondrites (lodranites, acapulcoites, winonaites, brachinites, and ureilites) (Fig. 2c), a fact suggesting that this olivine crystallized in the parent body of HED meteorites. However, even in diogenites, including olivine diogenites, olivine inclusions are more ferrous ( $Fo_{69}$ – $Fo_{79}$ ) (Hewins, 1981; Irving et al., 2005; Shearer et al., 2007). The most magnesian olivine was found only in the form of monomineralic fragments and in peridotite fragments in howardites (Lorenz et al., 2001). The composition of olivine of the high-Mg inclusions is comparable only with that of recently found dunite meteorites, which were genetically related to the parent body of HED meteorites: QUE93148 ( $Fo_{85.5}$ ; Goodrich and Righter, 2000) and NWA 2968 ( $Fo_{92.5}$ ; Bunch et al., 2006). The coarse-grained texture of the high-Mg olivine inclusions provides evidence of a low cooling rate and, hence, a significant depth at which the rocks occurred that served as the source of the fragments of high-Mg olivine. The pyroxene–chromite symplectites found in these inclusions have a composition and texture analogous to those of symplectites described in diogenites (Mittlefehldt, 2000; Irving et al., 2003), fragments of ultrabasic rocks in Dhofar 018 howardite (Lorenz et al., 2001), olivine chondrite QUE 93148 (Goodrich and Righter, 2000), and lunar rocks (Bell et al., 1975; McCallum and Schwartz, 2001).

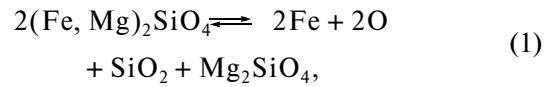
The results of computer simulations of the crystallization of chondritic melts, to which the genesis of HED meteorites can be related (Ruzicka et al., 1997; Righter and Drake, 1997; Lorenz et al., 1998), indicate that olivine of composition corresponding to that of high-Mg inclusions in Budulan, other mesosiderites, and dunite meteorites of the HED group was formed early in the crystallization process. Hence, such inclusions could be fragments of rocks produced by olivine sedimentation from chondritic melts. It is thus reasonable to suggest that the high-Mg olivine inclusions in Budulan can represent material from deeper levels in the differentiated parent body of HED meteorites (lower crust or upper mantle).

#### *Genesis of Veinlets in the Olivine Inclusions*

Veinlets accompanied by zoning likely resulted from secondary alterations analogous to those induced by hydrothermal–metasomatic processes. In essence, the secondary alterations of olivine inclusions in the Budulan meteorite were iron reduction under the effect of anhydrous fluid. The anhydrous nature of the fluid also follows from the absence of hydrous phases in the secondary alteration zones. Although no alterations of this type have never been detected in mesosiderites, they were documented in meteorites of some

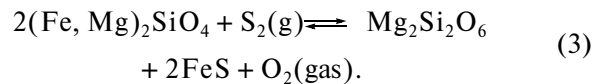
other types. For example, *in-situ* olivine reduction with the crystallization of metallic iron was documented in a number of EH3 chondrites (Matsunami and El Goresy, 1992; Weisberg et al., 1994). Enstatite chondrites show evidence of olivine sulfidization with the origin of sulfide, pyroxene, and silica (Rubin, 1984). The elevated Mg# of olivine in lodranites (primitive chondrites) along fractures could have resulted from reactions with S-rich fluid (Papike et al., 1995). In ureilites narrow zones of low-Fe olivine and to lesser extent, pyroxene are observed at the contacts with carbon-bearing matrix (Berhly et al., 1980). The increase in the Mg# and the replacement of olivine by a fine-grained aggregate of troilite and enstatite around sulfide veinlets were detected in lunar regolith 67016 and were thought to be caused by an olivine reaction with S-bearing vapor (Norman et al., 1991). Traces of olivine ( $Fo_{56}$ ) replacement by a fine-grained aggregate of troilite and enstatite ( $En_{65}$ ) in association with sulfide veinlets were found in the Dar al Gani 779 howardite. In this situation, again, it was thought that the secondary alterations resulted from a reaction of olivine with S-bearing vapor of, perhaps, impact genesis (Rosing and Haack, 2004). The texture and composition of this material are most closely analogous to those of olivine inclusions in Budulan.

When iron is reduced in the fayalite component of olivine [reaction (1)] and the resulted silica and forsterite recombine [reaction (2)], the olivine is replaced by an aggregate of magnesian pyroxene and Silica



The presence of silica in secondary aggregates around grains of secondary enstatite and metal or sulfide in Budulan suggests that silica could be partly prevented from participation in reaction (2).

The reduction of olivine under the effect of gaseous  $S_2$  at very high sulfur/olivine ratios was experimentally reproduced in (Kullerud and Yoder, 1963, 1964)



Reaction (3) was determined (Colson, 1992) to be independent of pressure, and the shift of this equilibrium to the right should be controlled by a decrease in the  $O_2/S_2$  ratio. This condition is fulfilled if the fluid has a very low initial  $O_2/S_2$  ratio or if this ratio decreases to a value sufficient for the reaction to proceed as the temperature (or pressure) decrease (Colson, 1992). As gas reactions controlling oxygen fugacity, Colson (1992) suggested the reactions

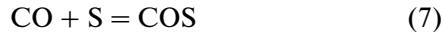


He has demonstrated that sulfide and enstatite in olivine can be synthesized by reactions with a mixture of CO, CO<sub>2</sub>, and S<sub>2</sub> (with this mixture containing approximately 0.6% S<sub>2</sub>) at temperatures of 800–1200°C. Hence, the effect of an sulfur-bearing gas with an oxygen fugacity controlled by the CO-CO<sub>2</sub> buffer can adequately account for the magnesian composition of the secondary associations of both the high-Mg and the low-Mg olivine. However, an increase in the Mg# of the olivine not coupled with the separation of metallic iron in the olivine suggests that iron should diffuse into fractures, in which it is mobilized and redeposited in the form of metal, which cannot be explained by Eq. (3). This reactions also fails to explain the occurrence of metallic iron in the mineral aggregates of types II and III.

As a mechanism responsible for the mobilization of metal and sulfides on the Moon, Colson (1992) considered the synthesis of carbonyl compounds of metals, such as Fe(CO)<sub>5</sub>, Ni(CO)<sub>4</sub>, and Cr(CO)<sub>6</sub>, which are stable within a broad temperature range and whose decomposition results in the redeposition of metals



and the synthesis of carbonyl sulfide (COS)



with this compounds subsequently reacting with metal carbonyls



The set of reactions presented above is able to generally adequately reproduce the secondary mineral associations in inclusions of the Budulan mesosiderite. The increase in the Mg# of olivine in the secondary alteration zones of the low-Mg inclusions (from Fo<sub>65</sub> to Fo<sub>78</sub>) is more intense than in the high-Mg inclusions (from Fo<sub>86</sub> to Fo<sub>93</sub>), and this allows us to correlate the amount of reduced iron with the initial fayalite mole fraction in the olivine. These observations indicate that the deposition of metallic iron in the aggregates of type I could brings about the aggregates of type II (troilite, metal, pyroxene, and silica). Hence, the aggregates of type I could be produced by reduction under the effect of an S<sub>2</sub>-bearing gas, while the aggregates of types II and III could be formed by the deposition of the metal mobilized in the aggregates of type I. Conceivably, the CO, CO<sub>2</sub>, and S<sub>2</sub> proportions in the fluid could vary. The small thicknesses of the zones in which olivine is replaced by metal–pyroxene–silica aggregates compared to the thicknesses of zones with pyroxene–troilite–silica aggregates seems to suggest a change in the diffusion rate, fluid mass, or the action time of this fluid.

The enrichment of the metal and sulfides in Ni in the secondary alteration zones suggest that Ni was borrowed from an external source, because metal reduced from the olivine should have been very poor in Ni. It is reasonable to suggest that Ni was more mobile

in a carbonate form and could be extracted from the metallic component of the meteorite. Metal veinlets cutting the altered and unaltered olivine and not accompanied by secondary alterations could be generated by the emplacement of impact melt, as was demonstrated in experiments on the shock load of mesosiderites (Rowan and Mittlefehldt, 1994).

### Sources of Fluid

Veinlets around which traces of metasomatism were identified in the low-Mg olivine continue into the host rock and, hence, should have resulted from fluid percolation along fractures through the already-formed breccia. This conclusion finds convincing supporting arguments in the fact that traces of metasomatic alterations were detected in olivine inclusions of various genesis that occur in association with one another only in the breccia of Budulan. Thermal metamorphism in the parent body of the Budulan mesosiderite should have redistributed FeO and MgO in the silicate and obliterate zoning in the altered olivine. Hence, the presence of this zoning suggests that the secondary alterations took place either simultaneously with the thermal metamorphism, which could induce and maintain fluid percolation, or after the termination of this process. Such gases as S<sub>2</sub>, CO, and CO<sub>2</sub> could be generated both by the impact evaporation of the target material or projectile and by endogenic processes in the interiors of the parent body. Melosh (1990) has demonstrated that impact vapor generated by an impact event partly moves toward the target at a high speed and enters cracks and fractures in the crater bottom. The source of vapor rich in sulfur and carbon compounds could be a projectile of cometary or CI composition. At the same time, the impact event could facilitate the mobilization of volatile components brought by earlier impact events or initiate the migration of endogenic fluid.

S<sub>2</sub> and CO are important components of terrestrial volcanic gases (Greenland, 1984). CO and CO<sub>2</sub> are the predominant volcanic gases (Housley, 1978; Sato, 1979; Wilson and Head, 1979). A lunar volcanic gas can additionally contain C–O–S compounds (Grove, 1981). An example of a planetary body with modern sulfuric volcanic activity and S<sub>2</sub> and SO<sub>2</sub> emissions is Io, a Jovian moon (Lopes et al., 2004; Jessup et al., 2005; Geissler, 2005; Schaefer and Fegley, 2005). This provides further arguments in support of the hypothesis of the endogenic nature of the fluid that has modified olivine inclusions in the Budulan mesosiderite.

An intense S<sub>2</sub> and CO flux could occur during the accretion and differentiation of primitive chondrite bodies and the origin of primitive achondrites. The source of such gases could be organic matter and sulfides of chondritic or cometary provenance. Metasomatic processes of this type could redistribute Fe in the interiors of the parent bodies and ensure the genera-

tion of highly magnesian deep-sitting material rich in pyroxene.

## CONCLUSIONS

The Budulan mesosiderite contains two types of olivine inclusions with different Mg# values. These inclusions originated from different sources in the parent body of HED meteorites.

The inclusions show traces of secondary alterations that resulted from the action of anhydrous gaseous fluid that moved along fractures and contained S<sub>2</sub>, CO, and CO<sub>2</sub>. The metasomatic processes reduced and removed iron in the form of its mobile carbonyl compounds.

These metasomatic alterations took place most probably after the origin of the breccia, under the effect of fluid that could be of either endogenic or supergenetic genesis.

It may be hypothesized that such reducing metasomatic processes could serve as an efficient tool of the fractionation of elements early in the process of differentiation of chondritic bodies, during the separation of sulfur and carbon-bearing compounds from the silicate material.

## ACKNOWLEDGMENTS

The authors thank the late Prof. Gero Kurat of the Museum of Natural History in Vienna, Austria, whose continuous efforts helped us in conducting this research. This study was financially supported by the AFW fund (Austria) and the Austrian Academy of Sciences.

## REFERENCES

- P. M. Bell, H. K. Mao, E. Roedder, and P. W. Weiblen, "The Problem of the Origin of Symplectites in Olivine-Bearing Lunar Rocks," *Lunar Sci. Conf.* **6**, 231–248 (1975).
- J. L. Berkley, G. J. Taylor, K. Keil, G. E. Harlow, and M. Prinz, "The Nature and Origin of Ureilites," *Geochim. Cosmochim. Acta* **44**, 1579–1597 (1980).
- J. S. Boesenberg, J. S. Delaney, and M. Prinz, "Magnesian Megacrysts and Matrix in the Mesosiderite Lamont," *Lunar Planet. Sci. Conf.* **28**, 125–126 (1997).
- T. E. Bunch, J. H. Wittke, D. Rumble, III, A. J. Irving, and B. Reed, "Northwest Africa 2968: Dunite from Vesta," *Meteorit. Planet. Sci.* **41** Suppl. Abstr. #5252 (2006).
- R. N. Clayton and T. K. Mayeda, "Oxygen-Isotope Studies of Achondrites," *Geochim. Cosmochim. Acta* **60**, 1999–2018 (1996).
- R. O. Colson, "Mineralisation on the Moon?: Theoretical Considerations of Apollo 16 'Rusty Rocks,' Sulfide Replacement in 67016, and Surface-Correlated Volatiles on Lunar Volcanic Glass," *Proc. Lunar Planet. Sci. Conf.* **22**, 427–436 (1992).
- J. S. Delaney, C. E. Nehru, and M. Prinz, "Olivine Clasts from Mesosiderites and Howardites: Clues to the Nature of Achondritic Parent Bodies," *Proc. Lunar Planet. Sci. Conf.* **11**, 1073–1087 (1980).
- J. S. Delaney, C. O'Neill, C. E. Nehru, M. Prinz, C. Stokes, H. Kojima, and K. Yanai, "The Classification and Reconnaissance Petrography of Basaltic Achondrites from the Yamato 1979 Collection Including Pigeonite Cumulate Eucrites, a New Group," *Proc. Ant. Met. Symp.* **9**, NIPR, **35**, 53 (1984).
- R. J. Floran, "Silicate Petrography, Classification, and Origin of the Mesosiderites: Review and New Observations," *Proc. Lunar Planet. Sci. Conf.* **9**, 1053–1081 (1978).
- M. J. Gaffey, "Surface Lithologic Heterogeneity of Asteroid 4 Vesta," *Icarus* **127**, 130–157 (1997).
- P. E. Geissler, "Volcanic Plumes and Plume Deposits on Io," *Lunar Planet. Sci. Conf.* **36**, #1875 (2005).
- C. A. Goodrich and J. S. Delaney, "Fe/Mg-Fe/Mn Relations of Meteorites and Primary Heterogeneity of Primitive Achondrite Parent Bodies," *Geochim. Cosmochim. Acta* **64**, 149–160 (2000).
- C. A. Goodrich and K. Righter, "Petrology of Unique Achondrite Queen Alexandra Range 93148: A Piece of the Pallasite (HED) Parent Body?," *Meteorit. Planet. Sci.* **35**, 521–536 (2000).
- L. P. Greenland, "Gas Composition of the January 1983 Eruption of Kilauea Volcano, Hawaii," *Geochim. Cosmochim. Acta* **48**, 193–195 (1984).
- T. L. Grove, "Compositional Variations among Apollo 15 Green Glass Spheres?," *Lunar Planet. Sci. Conf.* **12**, 935–948 (1981).
- R. H. Hewins, "Orthopyroxene-Olivine Assemblages in Diogenites and Mesosiderites," *Geochim. Cosmochim. Acta* **45**, 123–126 (1981).
- R. G. Hewins, "The Case for a Melt Matrix in Plagioclase-POIK Mesosiderites," *Proc. Lunar Planet. Sci. Conf.* 15th, *J. Geophys. Res.* **89** (15), C289–C297 (1984).
- R. M. Housley, "Modeling Lunar Volcanic Eruptions," *Proc. Lunar Planet. Sci. Conf.* **9**, 1473–1484 (1978).
- A. J. Irving, S. M. Kuehner, R. W. Carlson, and D. Rumble, III, A. C. Hupé, and G. M. Hupé, "Petrology and Multi-Isotopic Composition of Olivine Diogenite NWA 1877: A Mantle Peridotite in the Proposed HEDO Group of Meteorites," *Lunar Planet. Sci. Conf.* **36**, Abstr. #2188 (2005).
- A. J. Irving, S. M. Kuehner, D. Rumble III, A. C. Hupé, and G. M. Hupé, "Olivine Diogenite NWA 1459: Plumbing the Depths of 4 Vesta," *Lunar Planet. Sci. Conf.* **34**, Abstr. #1502 (2003).
- K. L. Jessup, J. R. Spencer, and R. Yelle, "Sulfur volcanism on Io," *Amer. Astron. Soc. DPS* 37th meeting, Abstr. #63.02 (2005).
- O. A. Kirova and M. I. D'yakonova, "Mesosiderite Budulan," *Meteoritika* **27**, 167–177 (1966).
- G. Kullerud, Yoder Jr., "Sulfide-silicate Reactions," *Carnegie Inst. Washington Yearbook*, 215–218 (1963).
- G. Kullerud, Yoder Jr., "Sulfide-Silicate Reactions," *Carnegie Inst. Washington Yearbook*, 218–222 (1964).

25. R. M. C. Lopes, L. W. Kamp, W. D. Smythe, P. Mouginis-Mark, J. Kargel, J. Radebaugh, E. P. Turtle, J. Perry, D. A. Williams, R. W. Carlson, S. Douté, "Lava Lakes on Io: Observations of Io's Volcanic Activity from Galileo NIMS during the 2001 Fly-Bys," *Icarus* **169**, 140–174 (2001).
26. C. Lorenz, G. Kurat, and F. Brandstaetter, "Mineral Chemistry of the Budulan Mesosiderite," in *Berichte der Deutschen Mineralogischen Gesellschaft*, 273 (1999).
27. C. Lorenz, M. Nazarov, G. Kurat, and F. Brandstaetter, "High-Magnesium Lithologies and Dry Fluid Metasomatism in the Budulan Mesosiderite," *Lunar Planet. Sci. Conf.* **31**, Abstr. #1315 (2000).
28. C. Lorenz, M. Nazarov, G. Kurat, F. Brandstaetter, and Th. Ntaflos, "Clast Population and Chemical Bulk Composition of the Dhofar 018 Howardite," *Lunar Planet. Sci. Conf.* **32**, Abstr. #1778 (2001).
29. B. Mason, "ALH85001," *Meteor. Bull.* No. 76, *Meteoritics* **29**, 100–143 (1994).
30. S. Matsunami and A. El Goresy, "Constraints to the Formation of Matrix Reduced Olivine in Yamato 691 (EH3) Chondrite: Implication for the Evolution of EH Chondrites," *Meteoritics* **27**, 256 (1992).
31. I. S. McCallum and J. M. Schwartz, "Lunar Mg Suite: Thermobarometry and Petrogenesis of Parental Magmas," *J. Geophys. Res.* **106** (E11), 27969–27983 (2001).
32. H. J. Melosh, *Impact Cratering: A Geologic Process* (Mir, Moscow, 1994; Clarendon Press, New York, 1989).
33. D. W. Mittlefehldt, "Petrographic and Chemical Characterization of Igneous Lithic Clasts from Mesosiderites and Howardites and Comparison with Euclites and Diogenites," *Geochim. Cosmochim. Acta* **43**, 1917–1935 (1979).
34. D. W. Mittlefehldt, "Petrology and Geochemistry of the Elephant Moraine A79002 Diogenite: A Genomic Breccia Containing a Magnesian Harzburgite Component," *Meteoritics Planet. Sci.* **35**, 901–912 (2000).
35. D. W. Mittlefehldt, D. D. Bogard, J. L. Berkley, and D. H. Garrison, "Brachinites: Igneous Rocks from a Differentiated Asteroid," *Meteor. Planet. Sci.* **38**, 1601–1625 (2003).
36. M. D. Norman, G. J. Taylor, and K. Keil, "Additional Complexity in the Lunar Crust—Petrology of Sodic Anorthosites and Sulfur-Rich, Ferroan Noritic Anorthosites," *Geophys. Res. Lett.* **18**, 2081–2084 (1991).
37. Th. Ntaflos, G. Kurat, C. Koeberl, and F. Brandstaetter, "Mincy Dunite F6241B: The Missing Ultramafic Component from Mesosiderites," *Meteorit. Planet. Sci.* **23**, 414 (1993).
38. J. J. Papike, M. N. Spilde, G. W. Fowler, G. D. Layne, and C. K. Shearer, "The Lodran Primitive Achondrite: Petrogenetic Insights from Electron and Ion Microprobe Analysis of Olivine and Orthopyroxene," *Geochim. Cosmochim. Acta* **59**, 3061–3070 (1995).
39. *Planetary Materials*, Ed. J. J. Papike, *Rev. Mineral.* **36**, 4–56–4–159 (1998).
40. M. Prinz, D. G. Waggoner, and P. J. Hamilton, "Winonaites: A Primitive Achondritic Group Related to Silicate Inclusions in IAB Irons," *Lunar Planet. Sci. Conf.* **11**, 902–904 (1980b).
41. M. Prinz, C. E. Nehru, J. S. Delaney, G. E. Harlow, and R. L. Bedell, "Modal Studies of Mesosiderites and Related Achondrites, Including the New Mesosiderite ALHA 77219," *Proc. Lunar Planet. Sci. Conf.* **11**, 1055–1071 (1980a).
42. K. Righter and M. Drake, "A Magma Ocean on Vesta: Core Formation and Petrogenesis of Euclites and Diogenites," *Meteorit. Planet. Sci.* **32**, 929–944 (1997).
43. M. T. Rosing and H. Haack, "The First Mesosiderite-Like Clast in a Howardite," *Lunar Planet. Sci. Conf.* **35**, Abstract #1487 (2004).
44. L. R. Rowan and D. W. Mittlefehldt, "More Shock Recovery Experiments on Mesosiderite Analogs," *Lunar Planet. Sci. Conf.* **25**, 1167–1168 (1994).
45. A. E. Rubin, "The Blithfield Meteorite and the Origin of Sulfide Rich, Metal Poor Clasts and Inclusions in Brecciated Enstatite Chondrites," *Earth Planet. Sci. Lett.* **67**, 273–283 (1984).
46. A. Ruzicka, G. A. Snyder, L. A. Taylor, "Vesta as the Howardite, Euclite and Diogenite Parent Body: Implications for the Size of a Core and for Large-Scale Differentiation," *Meteorit. Planet. Sci.* **32**, 825–840 (1997).
47. M. Sato, "The Driving Mechanism of Lunar Pyroclastic Eruptions Inferred from the Oxygen Fugacity Behavior of Apollo 17 Orange Glass," *Proc. Lunar Planet. Sci. Conf.* **10**, 311–325 (1979).
48. L. Schaefer and B. Fegley, Jr., "Predicted Abundances of Carbon Compounds in Volcanic Gases on Io," *Astrophys. J.* **618** (2), 1079–1085 (2005).
49. C. K. Shearer, P. V. Burger, and J. J. Papike, "Petrogenetic Relationships between Diogenites and Olivine Diogenites: Implications for Magmatism on the HED Parent Body," *Lunar Planet. Sci. Conf.* **38**, LPI Contrib. No. 1338, 1141 (2007).
50. E. Stolper, "Experimental Petrology of Eucritic Meteorites," *Geochim. Cosmochim. Acta* **41**, 587–611 (1977).
51. D. Terribilini, O. Eugster, and D. Mittlefehldt, L. Diamond, S. Vogt, and D. Wang, "Mineralogical and Chemical Composition and Cosmic-Ray Exposure History of Two Mesosiderites and Two Iron Meteorites," *Meteorit. Planet. Sci.* **35**, 617–628 (2000).
52. J. T. Wasson and A. E. Rubin, "Formation of Mesosiderites by Low-Velocity Impacts as a Natural Consequence of Planet Formation," *Nature* **318** (6042), 168–170 (1985).
53. J. T. Wasson, R. Shaudu, R. W. Bild, and C. Chen-Lin, "Mesosiderites—I. Compositions of Their Metallic Portions and Possible Relationships to Other Metal-Rich Meteorite Groups," *Geochim. Cosmochim. Acta* **38**, 135–149 (1974).
54. M. K. Weisberg, M. Prinz, and R. A. Fogel, "The Evolution of Enstatite and Chondrules in Unequilibrated Enstatite Chondrites: Evidence from Iron-Rich Pyroxene," *Meteoritics* **29**, 362–373 (1994).
55. L. Wilson and J. W. Head, "Ascent of Magma with Volatiles on the Earth and Moon," *Lunar Planet. Sci. Conf.* **10**, 1350–1352 (1979).